Relative Size of the Polymer and Nanoparticle Controls Polymer Diffusion in All-Polymer Nanocomposites

Halie J. Martin[1], B. Tyler White[2], Guangcui Yuan[3,4], Tomonori Saito[2], and Mark D. Dadmun[1,2*]

[1]Department of Chemistry, University of Tennessee, Knoxville, Tennessee 37996
[2]Chemical Sciences Division, Oak Ridge National Laboratory, Oak Ridge, Tennessee 37830
[3]NIST Associate Center for Neutron Research, National Institute of Standards and Technology, Gaithersburg, Maryland 20899
[4]University of Georgetown, Washington D.C. 20057

Abstract

The dynamics of polymers in an all-polymer nanocomposite that are composed of soft crosslinked polystyrene nanoparticles and linear polystyrene have been investigated. In this article, we describe how the relative size of the nanoparticle to that of the polymer chain and its rigidity impact the linear polymer chain diffusion. The results of the *in-situ* neutron reflectivity experiments show three distinct regimes in the linear polymer diffusion. The results indicate that the inclusion of soft nanoparticles increases the amount of topological constraints and confinement effects for low matrix molecular weight polymer. At modest molecular weights where the size of the nanoparticle and polymer chain are similar, the soft nanoparticles neither inhibit nor enhance the linear polymer diffusion, while at the highest polymer matrix molecular weight, the linear polymer diffusion increases due to an increase in the constraint release mechanism by the soft nanoparticles. Thermal analysis shows that the nanoparticles do not increase the free volume of the system nor do they behave as a plasticizing agent. These results are interpreted to indicate that the competition between a topological barrier effect and enhancing constraint release defines the behavior of a given all-polymer nanocomposite.

Introduction

Polymer nanocomposites have recently become an important construct in the development and application of novel functional materials. The homogeneous dispersion of nanoparticles into polymer matrices is needed to realize targeted improvement in material properties, where this dispersion is dependent on the polymer/nanoparticle interactions.[1] Moreover, knowledge of polymer mobility in a nanocomposite is essential to understand and the optimize a variety of properties of the nanocomposite, including adhesion, crack healing, and welding applications.[2] The inter-diffusion of polymer chains is usually strongly impeded as a result of incorporation of hard impenetrable nanoparticles. On the other hand, the addition of polymeric, organic nanoparticles to a linear polymer matrix has resulted in unique dynamic behavior, including significant viscosity reduction as well as increased polymer diffusion in polystyrene nanocomposites.[3,4] Therefore, understanding and monitoring the dynamics of linear chains in these all-polymer nanocomposites provides insight into the role of the soft nanoparticle on the dynamics of the linear polymer matrix.

Monitoring thin film polymer inter-diffusion provides a mechanism to examine the mobility of the polymer chains across joined layers of bulk polymer.[5,6] The initial layers are immobile and unable to move across the layer interface, however, when the polymer layers are heated above the glass transition temperature of the polymer, the polymer chains diffuse across the bilayer interface. For polymers that are entangled, i.e. above the critical molecular weight for the polymer, the most successful model to describe such polymer dynamics is the reptation model.[2,7,8] In this tube model, the polymer chain is trapped within a fictitious tube with radius a, where the tube is a representation of topological restraints from neighboring polymer chains or nanoparticles. The polymer chain motion is severely restricted laterally by the tube radius. In this model, the

initial polymer motion can be described as Brownian motion that follow Rouse dynamics where segmental motion can be monitored.[9,10] During these short time motions, the interaction of the polymer with the surrounding medium is by a cumulative friction between the surroundings and the polymer. For longer time scales in entangled polymers where the polymer chain moves distances greater than their own radius of gyration, the dynamics of the chains are dominated by the reptation model.[11,12,13]

To understand how bulk polymer diffusion is affected by the inclusion of nanoparticles, researchers have used a wide range of scientific techniques including elastic recoil detection, rheology, Raman microscopy, Rutherford backscattering spectrometry, Fourier transform infrared spectrometry, and neutron reflectivity. [3,4,14–20] A common protocol to monitor polymer inter-diffusion is to create a polymer bilayer where one layer is composed of protonated polymer and the second layer consists of deuterated polymer with symmetric molecular weights. The deuteration of one layer provides contrast for neutron reflectivity,[21] NR, which provides a perpendicular composition profile at the polymer-polymer bilayer with nanoscale resolution.[2] Using this geometry, neutron reflectivity has successfully monitored short and long relaxation processes at the polymer-polymer interface.[4,10,13,20,22,23] Traditional reflectivity experiments that monitor the broadening of the polymer-polymer interface with diffusion usually involves an anneal-quench experimental procedure where a sample is heated above the bulk glass transition temperature, T_g, for a specific period of time in an oven. The sample is then rapidly quenched below room temperature to halt polymer motion thus immobilizing the polymers. The samples are then characterized by neutron reflectivity in this frozen state. This method can result in many experimental difficulties such as slow quenching that will disturb the polymer-polymer interface, uneven heating or quenching of the sample, as well as destroying the sample from human error.

These static measurements also make it difficult to detect the initial inter-diffusion of the smaller molecular weight polymers, leading to increased experimental uncertainty. Bucknall et al designed a "time-resolved" approach to monitor the diffusion of polystyrene, PS, bilayers by outfitting the NR sample stage with a thermostatically heatable brass plate.[23] This modified sample stage allowed for real-time reflectivity measurements over a modified Q-range of 0.008 to 0.08 Å^{-1}, where Q = $^{4\pi}/_{\lambda}$ sin (θ), to monitor the change in the interfacial width of a symmetric neat PS bilayers in-situ as the sample was heated above its glass transition temperature. These experiments demonstrate that at short times, t, the interfacial width increases as $t^{1/4}$, which is indicative of Rouse dynamics. This interfacial width dependence transitions from $t^{1/4}$ to $t^{1/2}$ for times greater than the $\tau_{reptation}$, where Fickian diffusion dominates the growth of the interfacial width. The rate of the growth of the interfacial width, w, is then analyzed to extract a mutual diffusion coefficient of the two polymers, $w = (4Dt)^{1/2}$.

The recent growth of nanocomposites research has led to a significant increase in the interest of the diffusion behavior of polymers in the presence of nanoparticles. Nanoparticles are of particular interest due to their high interfacial surface area which has a stronger influence on the dynamics of a polymer system and are capable of improving the mechanical, thermal, electrical and optical properties of the composite.[1,24–32] By incorporating nanoparticles into a polymer matrix, even at low percentages, the bulk materials exhibit significantly different dynamic properties relative to those of the neat polymer. Generally, the dynamics of polymers in the presence of nanoparticles depend on a set of key length scales including radius of the nanoparticle, radius of gyration of the polymer matrix, R_g, and interparticle spacing between nanoparticles, ID.[14] Most nanocomposites of interest incorporate hard, inorganic nanoparticles which act as impenetrable obstacles that cause polymer diffusion to slow down due to the nanoparticles being

stationary barriers that add topological constraints to the motion of the polymer chains.[31–34,35] Recently, the addition of hard nanoparticles into a polymer matrix has been shown to decrease the diffusion of the linear polymer where even low loadings of spherical nanoparticles reduce the room the polymer has to move. This confinement effect, or constraint, is quantified by the interparticle spacing or ID_{eff}, a measure of the average distance between nanoparticles.[36] These results indicate that the molecular weight of the matrix, as well as polymer-nanoparticle interactions have a smaller effect on the slowing of polymer dynamics than *ID*, where the concentration of the nanoparticle and the particle size define ID_{eff} and therefore dominate the modified polymer dynamics.[32–34,37] Even grafted nanoparticles that exhibit a hard core but have a corona of penetrable grafted polymer chains exhibit a decrease in the rate of polymer diffusion that follow this model.[14]

However, incorporating soft single-chain polymer nanoparticles, SCPNs, in a polymer matrix appears to eliminate the undesired confinement effects of impenetrable hard nanoparticles. These single-chain polymer nanoparticles do not confine the polymer as with hard core nanofillers, but contribute primarily to the topological constraints of the diffusing chain.[1] For example, Mackay et al[38] investigated a system of crosslinked polystyrene nanoparticles in a polystyrene matrix in which the nanoparticle/polymer interactions essentially eliminate enthalpic dispersion forces. Incorporating the crosslinked nanoparticles into a chemically matched polymer matrix resulted in a reduction in viscosity compared to that of the neat polymer.[38] This phenomenon deviates from the Stokes-Einstein model[39] which predicts an increase in viscosity with nanoparticle loading. Bačová et al utilized simulations to model SCNPs in an ideal, all-polymer nanocomposite. This work determined that polymer matrix chains can fully penetrate crosslinked nanoparticles concluding that the change in the friction coefficient experienced by the linear chains is negligible with the inclusion of soft nanoparticles.[1]

The diffusive behavior of all-polymer nanocomposites has not been as extensively studied and is not well understood due to the complexities of the system and experiments. Previously, Miller et al determined that penetrable polystyrene soft nanoparticles increased the diffusion rate of linear polystyrene, where the extent of the increase is dependent on nanoparticle rigidity.[4] These experiments were completed for a system when the radius of gyration of the linear polymer is greater than that of the soft nanoparticle.[4] The increase in the diffusion of the linear polymer chains was interpreted to indicate that the unique topology of the nanoparticles, a well-defined crosslinked core with a corona comprised of chain ends and loops, enables an increase in the constraint release mechanism. This increase in the constraint release mechanism is similar to the effects observed with the addition of star polymers to a linear chain melt.[4,40] Within these systems, the shorter arms of the star polymers relax on a time scale faster than the reptating chain dilating the tubes for the unrelaxed chains. Imel et al also determined that the soft nanoparticles are not stationary in the polymer matrix and therefore their mobility may couple with the diffusive behavior of the linear polymer chains.[20]

The increased complexity of polymer diffusion of an all-polymer nanocomposite demonstrates the need for greater understanding of how topologically controlled soft, polymer nanoparticles affect the center of mass diffusion of linear polymer chains. In this article, in-situ time-resolved neutron reflectivity is completed to gain an understanding of how the presence of the soft nanoparticles affects the diffusion of linear polystyrene, PS, as a function of PS molecular weight. For this set of soft nanoparticles, the measured diffusion coefficients of neat polystyrene and polystyrene with a 1 wt % loading of soft PS nanoparticles are reported as a function of three PS matrix molecular weights. The presence of soft nanoparticles results in three distinct regimes for linear PS diffusion: for the lowest molecular weight (61kDa) matrix, all nanocomposites

exhibit a decrease in linear polymer diffusion coefficients, the middle molecular weight (215kDa) matrix exhibited very little change in the PS diffusion coefficients compared to that of the neat polymer, and the nanocomposites at the highest PS matrix molecular weight (540kDa) increased the diffusion coefficients of the linear polymer chain.

Experimental

Silicon wafers, 2-inch diameter with 5 mm thickness or 4-inch diameter with 1 mm thickness, were cleaned in a piranha solution composed of a 3:1 ratio of sulfuric acid and 30% hydrogen peroxide for 24 hours at 105 °C. Wafers were rinsed thoroughly with nanopure water and dried under a stream of nitrogen gas. The Si wafers were then placed in a Jelight UVO Cleaner for 15 minutes to complete removing any residual organic residue and to reform the oxide layer on the surface of the wafers.

A series of symmetric molecular weights of protonated polystyrene, h-PS, and deuterated polystyrene, d_8-PS, were purchased from Polymer Source Inc. with number average molecular weights, M_n, of 61,500/61,500, 211,000/215,000, and 535,000/540,000 g/mol respectfully and were used without further modification. Solutions of 1 wt% h-PS and d_8-PS in toluene were prepared for each polymer to cast films. Polymer bilayers were prepared by spin casting an h-PS film bottom layer onto a 2-inch reflectivity silicon wafer with thicknesses of 500-700 Å measured by laser ellipsometry. The bottom h-PS layers were dried overnight in a Lindberg Blue M vacuum oven at 130 °C to remove any excess solvent. Top layers of d_8-PS were prepared using the same spin coating method on a 4-inch thin silicon wafer. The d_8-PS layers were then floated off the silicon wafer onto the surface of nanopure water. The d_8-PS floated layer was picked up using the h-PS reflectivity wafer to create the neat bilayer geometry. The bilayers were then placed into a

vacuum oven at room temperature for a minimum of 24 hours to remove all excess solvent and residual nanopure water between the layers.

Soft polystyrene nanoparticles for this study were synthesized using a monomer-starved semi-batch nanoemulsion polymerization, the details of which can be found in the literature.[41] Careful neutron scattering results indicate that these nanoparticles consist of a well-defined crosslinked core with a corona that is comprised of chain ends and loops, resulting in a fuzzy interface between the nanoparticle and its surroundings. A list of relevant physical characteristics of the nanoparticles used in these studies can be found in Table 1. Nanocomposite bilayers were prepared using the same method with a 1 wt % loading of soft nanoparticle NP1, NP2, NP3, or NP4 in both linear polystyrene layers. The softness of the nanoparticles was controlled by the amount of divinylbenzene (DVB) crosslinker added during the emulsion polymerization. As the crosslinking density increases from 0.81% (NP1), 1.91% (NP2), 4.60% (NP3), to 10.7% (NP4), the nanoparticles become more rigid and the size of the corona/fuzzy interface decreases.

Table 1: Structural characteristics of the polystyrene soft nanoparticles used in the neutron reflectivity studies. All values were determined using small angle neutron scattering as previously reported.[41]

Soft NP Name	% DVB	R_g (Å)[a]	R_c (Å)[b]	τ_{fuzzy} (Å)[d]	R_p (Å)[e]	σ[f]
NP1	0.81	101 ± 0.5	34.66 ± 0.1	46.2 ± 1	126.9 ±.2	0.36 ± 0.03
NP2	1.91	68.3 ± 0.3	61.5 ± 17	24.88 ± 10	111.1 ± 26	0.22 ± 0.1
NP3	4.60	70.0 ± 0. 2	60.0 ± 2	14.0 ± 1	88.0 ± 1	0.16 ± 0.1
NP4	10.7	64.6 ± 0.1	7.05 ± 1	-	70.5 ± 4	-

[a] Divinylbenzene crosslinking mol% [b] Radius of gyration determined from the Guinier Analysis of SANS; [c] Radius of the soft nanoparticle core; [d] Half-width of fuzzy interfacial layer; [e] Total nanoparticle radius = $R_c + 2*\tau_{fuzzy}$ [f] Effective fuzziness of the nanoparticle $\sigma = \tau_{fuzzy}/R_p$

In-Situ Neutron Reflectivity

In-situ neutron reflectivity experiments were conducted at the National Institute of Standards and Technology Center for Neutron Research on the NG7 Horizontal Neutron Reflectometer. All reflectivity experiments were conducted in the NG7 Reflectometer Heated Pressure Vessel for Thin Films. This in-situ temperature chamber offered precise control of the temperature of the sample using a Peltier temperature controller controlled through LabVIEW software. The design of this cell provides a temperature evolution profile with very little overshoot and minimal fluctuation when the temperature was increased from 90 °C to 130 °C. As shown in Figure 1, under vacuum, the temperature chamber reaches a stable and constant temperature in under 5 minutes.

In the completion of the reflectivity experiments, the reflectivity curves of all as-cast samples were first obtained at 90 °C, below the glass transition temperature of neat polystyrene. The temperature was then increased to 130 °C, where the reflectivity of the samples is monitored. To anneal samples with 215 kDa and 540 kDa matrix molecular weights, a temperature ramp from 90°C to 130 °C was performed under vacuum and the reflectivity curves were then measured as a function of annealing time at 130 °C. This protocol results in time-resolved annealed reflectivity profiles, which were captured continuously for 4 hours with auto-alignment and continuous data capture every 13 minutes. However, this protocol is insufficient for the 61 kDa PS matrix as the polymer diffuses too quickly such that the important changes in the interfacial width occur within the first 15 minutes of the annealing process. The protocol was modified to include heating the sample in the in-situ chamber to 130 °C and annealing the sample for 3 minutes. The temperature was then quickly quenched back to 90 °C and the reflectivity profile was captured at 90 °C. This procedure was then repeated for 3-minute heating intervals at 130 °C up to a total annealing time of 15 minutes.

The reflectivity experiments were completed with a neutron wavelength, λ, of 4.75 Å and a *Q* range of 0.008 – 0.08 $Å^{-1}$. The reflectivity was then plotted as a function of the momentum transfer vector perpendicular to the reflection surface, $Q = (4\pi/\lambda)\sin\theta$, where θ is the angle of incidence. The reflectivity profiles, (*R*) vs *Q* (A^{-1}), were reduced using Reflpak software as well as online data reduction through the NIST website. The Motofit analysis package in IGOR Pro was used to fit reflectivity profiles to produce a scattering length density profile. Reflectivity profiles were fit by systematically varying the thicknesses of each layer, scattering length densities, and interfacial roughness until the best fit was achieved by optimizing the χ^2 parameter. To verify the validity of the reflectivity fits, the area under the scattering length density, SLD, profile was calculated and confirmed to not vary by more than 10% for all annealing times.

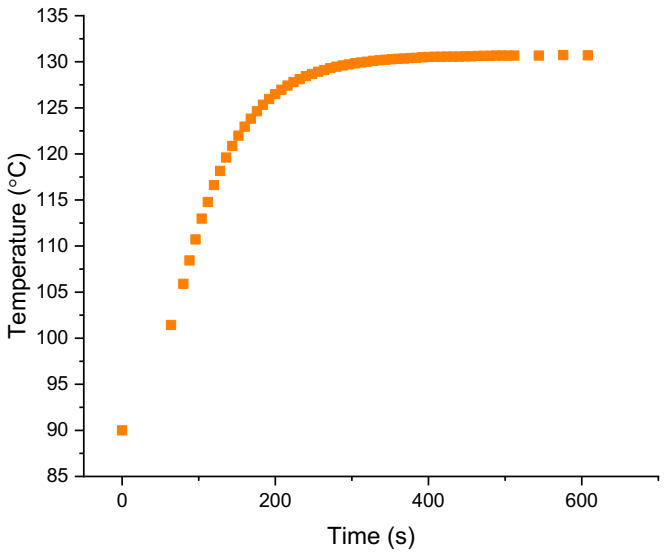

Figure 1: In-Situ temperature ramp from 90 °C to 130 °C.

Differential Scanning Calorimetry

The glass transition temperatures of the neat 540 kDa h-PS films and 540 kDa PS matrix nanocomposites were measured by differential scanning calorimetry using a TA Instruments Q1000 DSC with samples in standard sealed aluminum pans. The mass of the samples in aluminum pans were measured using Cahn C-33 Microbalance. The DSC procedure included a temperature ramp from 40 °C to 150 °C at 10 °C/minute and was repeated 4 times. The temperature curves were analyzed using TA Instruments' Universal Analysis software to calculate the glass transition temperature and standard deviation for all samples.

Results

Reflectivity profiles of the 540 kDa neat PS bilayer for a range of annealing times are presented in Figure 2 as an example of the changes in the reflectivity data with polymer diffusion at the polymer interface over time. The pink circles represent data collected for the as cast sample at 90 °C. The height of the reflectivity fringes for the as cast data correspond to a sharp interface in the sample, while the tall fringes that include two peaks are indicative of two distinct layers within the measured sample. The purple triangles are representative of the 540 kDa neat bilayer annealed at 130 °C for 1006 s and the blue squares is the bilayer annealed for 8051 s. The annealed curves show dampening of the fringes due to increased breadth of the PS:dPS interface thus representing the inter-diffusion of the two polymers at this interface. From the best fit of the reflectivity profiles, the scattering length density profiles of each sample are shown in Figure 3. Analysis of the as cast SLD curve (pink) in Figure 3 shows that the interface between the two layers at approximately 600 Å from the air interface exhibits a nearly vertical transition between the d_8-PS layer and h-PS layers. As the sample is annealed for longer times (purple 1006 s and blue 8051 s), the transition between layers becomes broader as a result of the two layers inter-

diffusing together. The SLD profiles of the annealed samples in Figure 3, also show an increase in overall bilayer thickness, which is a result of the kinetic trapping of the as-cast sample during spin coating, followed by their relaxation toward an equilibrium thickness when annealed at 130 °C.

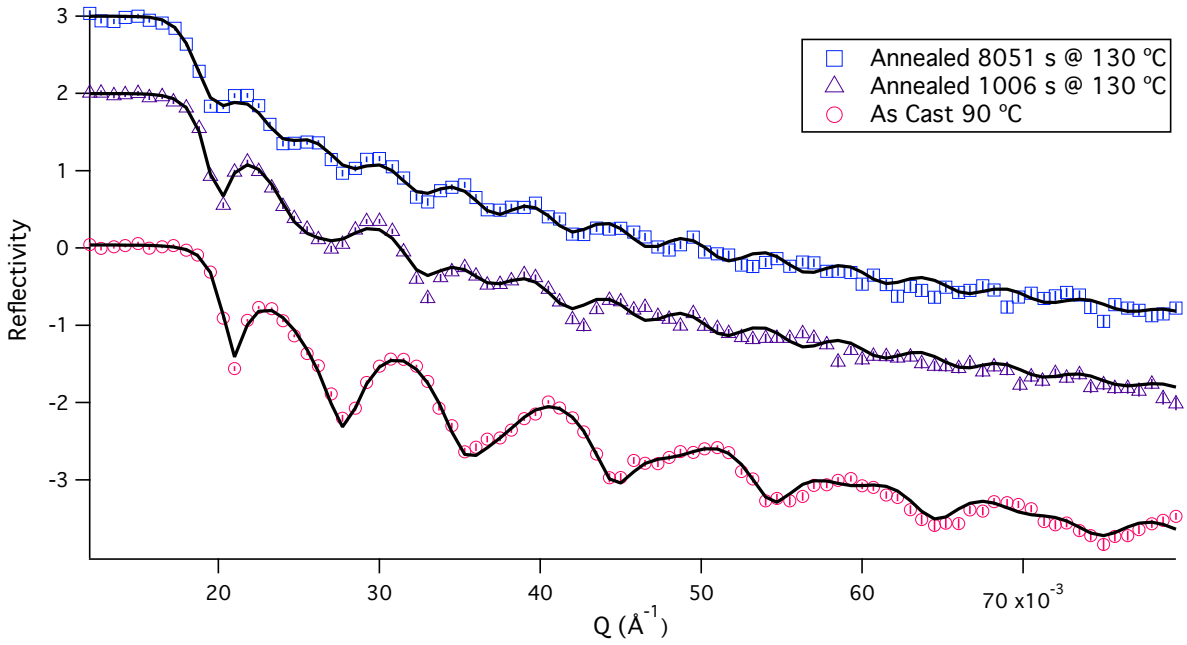

Figure 2: Reflectivity profiles for 540 kDa neat bilayer as a representation of all samples. The profiles are offset for clarity.

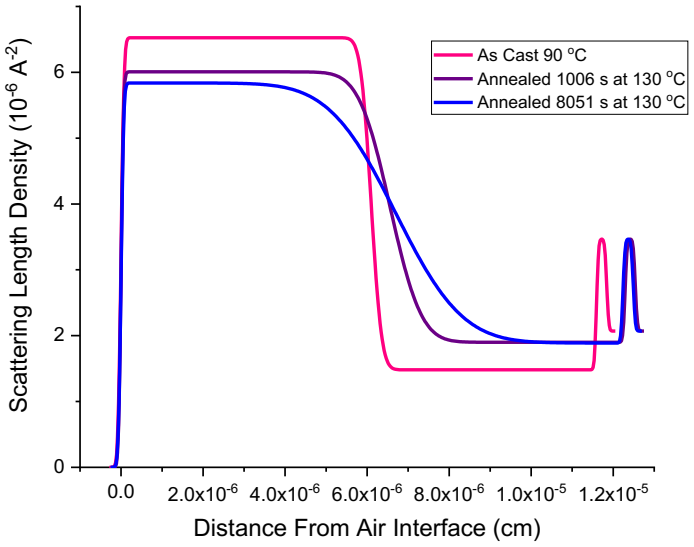

Figure 3: Scattering length density, SLD, curves for 540 kDa neat bilayer as a function of bilayer depth and annealing time at 130 °C where 0 is the air interface.

The SLD profiles are converted into a d_8-PS volume fraction profile using Equation 1. In Equation 1, ϕ_{dPS} is the d_8-PS volume fraction, SLD_m is the measured SLD at a given depth,

$$\phi_{dPS} = \frac{SLD_m - SLD_D}{SLD_D - SLD_H} \quad \text{Eq. 1}$$

SLD_D is the SLD of the pure deuterated PS, and SLD_H is the SLD of the pure protonated PS. The d_8-PS volume fraction profiles are then fit to a modified Fick's second law[10], Equation 2, to

$$\phi_{dPS} = \frac{1}{2} \times c \times erf\left[\frac{h-x}{w}\right] + b$$

Eq. 2 calculate the interfacial width as a function of annealing time. In Equation 2, *c* is a constant, *erf* is the error function, *h* is the thickness of the d_8-PS layer, *w* is the interfacial width, and *b* is the background. The depth profile of the 540 kDa neat bilayer after annealing for 8051 s at 130 °C is fit to Fick's second law, and is denoted by the solid black line in Figure 4. The determined interfacial widths are then plotted as a function of annealing time, as shown in Figure 5. In Figure 5, the time dependency of the growth in the interfacial width is fit to a power law. This analysis

shows a time dependence of $t^{1/4}$ at early times, which is consistent with Rouse dynamics. At later times, the time dependence of the interfacial width changes to follow Fickian diffusion, $t^{1/2}$. This time dependence is fit to Equation 3 where D is the diffusion coefficient and t is the annealing time.

$$w = (4Dt)^{1/2} \quad \text{Eq. 3}$$

This analysis produces a diffusion coefficient value of D = 9.4x10^{-17}cm^2/s for the 540 kDa neat bilayer. As a self-consistent check, the time at which the dynamics change from Rouse dynamics to reptative dynamics is calculated with Equation 4 using this diffusion coefficient. In this Equation, τ_r is the reptation time, N is the degree of polymerization, b is the segment length of polystyrene (6.7 Å), and D is the measured diffusion coefficient.[23] This analysis estimates that τ_r is equal to 7803 s for the 540 kDa neat bilayer, which is in reasonable agreement with the data in Figure 5.

$$\tau_r = \frac{Nb^2}{3\pi^2 D} \quad \text{Eq. 4}$$

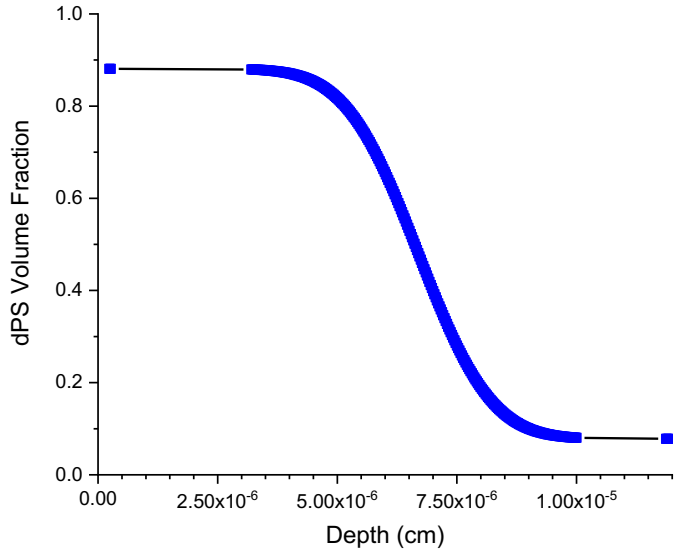

Figure 4: d_8-PS volume fraction fit (black line) for 540 kDa neat bilayer annealed for 8051s to a single error function to calculate interfacial width.

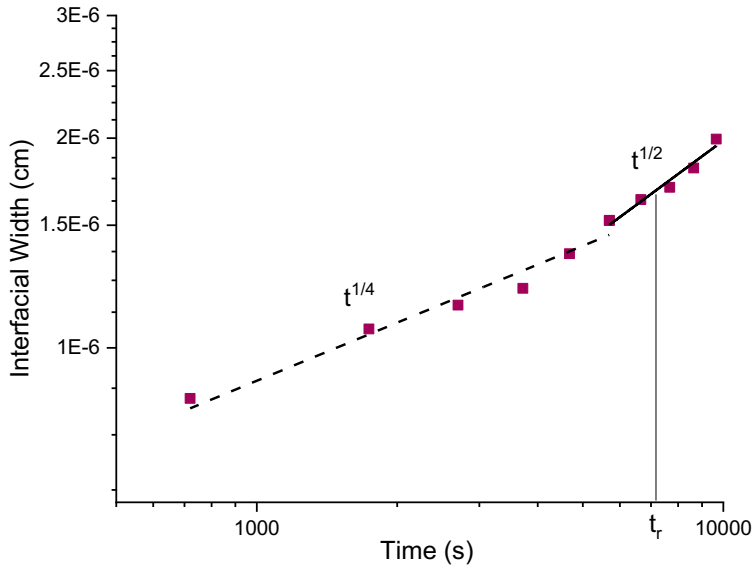

Figure 5: Log-log plot of interfacial width vs annealing time for 540 kDa neat bilayer reflectivity. The dashed line is fitted to the Rouse regime where there is a time dependency of $t^{1/4}$ and the solid line is fitted to the reptative regime where the time dependency is equal to $t^{1/2}$. The transition from Rouse dynamics to reptative dynamics is estimated by t_r.

This analysis protocol is used to determine the diffusion coefficients for all samples. The diffusion coefficients of the neat PS bilayers and nanocomposites containing the nanoparticles listed in Table 1 are plotted in Figure 6 as a function of linear polymer molecular weight. The uncertainty in each diffusion coefficient is smaller than the symbol. The neat PS diffusion coefficients systematically decreases with increasing PS molecular weight, following the expected $\sim Mw^{-2}$ dependence. For the nanocomposites with a 61 kDa matrix, the diffusion of the polystyrene in the nanocomposites is much *slower* than that of the neat PS polymer diffusion. Interestingly, the rate of diffusion of the 215 kDa PS in the nanocomposites do not change much from that of

the pure 215 kDa polymer. Finally, the diffusion of the 540 kDa PS in the nanocomposites diffuses much *faster* than that of the neat 540 kDa PS.

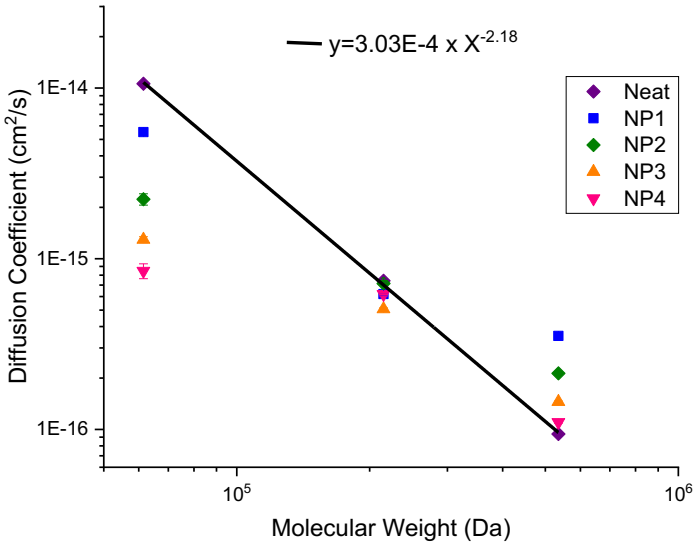

Figure 6: Molecular weight dependence of the measured diffusion coefficients for the neat bilayers and each nanocomposite as a function of molecular weights. The solid line is consistent with reptation theory molecular weight dependency for the neat bilayers.

Discussion

Hard, inorganic, spherical nanoparticles with no affinity to the matrix material will often aggregate and act as dense fillers, where they diminish the properties of the bulk matrix.[42–44] Well dispersed hard nanoparticles decrease polymer diffusion in a nanocomposite, due to an increase in confinement of the polymer chain between the small nanoparticles.[32] The impenetrability of these hard nanoparticles results in the confinement of the matrix polymer chains between neighboring nanoparticles, which decreases the entropy of the polymer chain, even at low nanoparticle loadings.[14,45-50] The surfaces of hard nanoparticles are often modified by grafting polymer chains onto the nanoparticles to counteract their aggregation in polymer matricies.[14,32–34] Moreover, studies show that the presence of these grafted nanoparticles with hard impenetrable cores also

slow the linear polymer diffusion. Composto and coworkers have shown that the polymer diffusion can be scaled to a universal curve based on the confinement parameter $ID/2R_{g(polymer)}$.[14] The universal confinement represents the ratio of the average distance between the surfaces of neighboring hard nanoparticles and the diameter of the polymer molecule. The interparticle distance, *ID*, is defined in Equation 5.[14,33] In Equation 5, *R* is the average radius of the nanoparticle and ϕ_{NP} is the volume fraction of the nanoparticles.

$$ID = 2R[\left(\frac{2}{\pi \times \phi_{NP}}\right)^{\frac{1}{3}} - 1] \quad \text{Eq. 5.}$$

In these systems, the polymer chain loses conformation entropy when it is confined between neighboring nanoparticles, thus the polymer chain continuously probes its surrounding environment until a large enough opening is found to reptate through. These added constraints to the polymer motion from the hard nanoparticle significantly slow polymer diffusion.[15]

Previous research has also examined systems where the dynamic response of a polymer chain increases with the incorporation of the nanoparticle.[35,51-53] The interpretation of these results to explain this behavior varies among researchers. Many of these results employ a dependency on the ratio of a characteristic length scale of the nanoparticle, i.e. diameter or radius of the nanoparticle, to a size of the polymer chain. For instance, Grabowski et al[35] infers that the inclusion of gold nanoparticle with diameters that are comparable or smaller than the tube diameter of the matrix polymer, poly(n-butyl methacrylate), decreases the friction coefficient between nanoparticle and polymer chains. When the relative size of the particle and the polymer tube diameter are similar, it is put forward as a crossover point between slower and faster dynamics of the polymer matrix.[35] Moreover, their reported viscosity reduction should correspond to an increase in polymer diffusion coefficient. When SCNPs with a diameter smaller than the Edwards tube diameter of the melt polymer are mixed with the polymer chains, there exists a dynamic

coupling between the nanoparticles and the polymer chains.[51] When the radius of the SCNP, R_a, is much smaller than the R_g of the matrix polymer, the segmental relaxation of the linear melt chains can be accelerated by the softness of the interface of the nanoparticle.[52,53] Therefore, the ratio of the size of the nanofiller to the radius of gyration of the bulk polymer is an important parameter that should qualitatively alter the dynamics of a polymer in a nanocomposite, as is observed on our results.

While there are many studies that examine the dynamics of linear polymers that are similar or smaller than the nanoparticle, there are few studies that examine nanocomposites systems with linear polymers that are 2 orders of magnitudes *larger* than the nanoparticle or nanocomposites comprised of single-chain nanoparticles dispersed in a linear polymer matrix. Miller et al examined the diffusion of large linear polystyrene in the presence of small soft polystyrene nanoparticles and observed a dramatic increase in linear polymer diffusion when the $R_{g(dPS)} \approx 2 \times R_{g(NP)}$. It is important to emphasize that the increase in dynamics is not merely an increase in free volume or a plasticizing effect with the incorporation of the nanoparticles.[4,20] These results demonstrate that the ratio of the $R_{g(NP)}/R_{g(polymer)}$ is important in determining the coupling of the presence of the nanoparticle to polymer motion, and deserves more in-depth study to understand the diffusion of linear chains in all-polymer nanocomposites.

Arbe *et al.*[31] determined that when the $R_{g(polymer)}$ is larger than the radius of single chain nanoparticles, SCNPs, the SCNPs dilate the tube diameter of the linear chain. This dilation decreases the lateral restrictions of the reptating tube. This result is consistent with the observed viscosity reductions by Mackay *et al.*[38] indicating increased dynamics for an all-polymer nanocomposite with soft interfaces. Overall, reported results indicate that the unique interfaces

provided by the topology of these SCNPs contribute to the singular dynamics and viscoelastic properties of all-polymer nanocomposites.[1,4,20,31,38,52]

The softness of the polymeric nanoparticles used in this work are defined by the amount of DVB crosslinker in their synthesis. Due to the chemical similarity of the nanoparticle and the polymer matrix, limited nanoparticle aggregation is expected or observed. It should be emphasized that the neutron reflectivity data indicates that the nanoparticle is homogeneously dispersed through the thickness of the film, i.e. there is no excess nanoparticle found at any interface. It has also been demonstrated that the diffusion of linear polymers in the presences of these soft PS NPs of this nature do not follow the universal scaling that is observed for polymer diffusion in the presence of hard impenetrable NPs.[57] Moreover, experimental results imply that these nanoparticles deform, which can aid the linear polymer diffusion, a mechanism that is not available for hard impenetrable nanoparticles.[20]

Diffusion of Polystyrene Nanocomposites: 61kDa PS Matrix ($R_{g(NP)} > R_{g(dPS)}$)

The first system studied is the matrix of low molecular weight polystyrene, ~ 61,000 Daltons and the corresponding nanocomposites. The radius of gyration for the 61 kDa polystyrene matrix is approximately 64 Å, which is estimated using Equation 6. In Equation 6, M_w is the weight average molecular weight for dPS, M_0 is the molar mass of the repeat unit (112 Da), and a is the segment length which is 6.7 Å for polystyrene.[4] This calculated value is slightly larger

$$R_g = \frac{a\sqrt{M_w/M_0}}{\sqrt{6}} \qquad \text{Eq. 6}$$

than the experimentally determined R_g of polystyrene with similar molecular weight using small angle neutron scattering by Mackay et al of 57 Å.[56] This $R_{g(dPS)}$ is smaller than that of the $R_{g(NP)}$ that is measured using small angle neutron scattering for the soft nanoparticles studied and reported in Table 1. The matrix molecular weight of 61,000 Da is well above the entanglement molecular

weight of the polymer, and is therefore entangled.[2,7,58] The diffusion of linear polystyrene decreases in the nanocomposites relative to that of neat polystyrene and decreases as the rigidity of the nanoparticle increases. The measured diffusion coefficient for the neat 61 kDa PS bilayer is 1.1×10^{-14} cm^2/s with a $\tau_{reptation}$ equal to approximately 7.8 seconds when annealed at 130 °C. At this temperature and neutron reflectivity time scales, the Rouse regime is not experimentally measurable.

The decrease in the linear PS diffusion rate is interpreted to be the result of the presence of the added nanoparticles increasing the barriers to the motion of the polymer chain. The diffusion coefficient for PS decreases by 2, 5, 8, and 12 times with the addition of 1 mass % loading of nanoparticles NP1, NP2, NP3, and NP4 respectfully, indicating that an increase in the crosslink density or rigidity of the nanoparticle enhances the attenuation of the polymer diffusion (Figure S 1-5). As the crosslinking density of the nanoparticle increases, the deformability of the nanoparticle decreases and the nanoparticle becomes more impenetrable.[59] This translates into more barriers on the diffusive motion of the polymer chain,[59] which manifests as a greater decrease in the measured diffusion coefficient.

The small molecular weight of the linear PS also means that more chain ends exist within the system relative to larger molecular weight PS. The presence of these chain ends offers more avenues for the polymer chain to diffuse and reptate into and become entangled within the deformable nanoparticle. As the nanoparticles move more slowly than the linear chains, this entanglement will also cause the polymer diffusion to slow down. When the nanoparticle becomes more crosslinked, the polymer chains become more confined. This, in turn, further reduces the diffusive motion of the polymer chain.

The reduced motion of the 61 kDa PS diffusion in the presence of the nanoparticles is, therefore, attributed to the nanoparticles acting as barriers to the diffusion of linear polymer chains and the entanglement of the linear chain with the nanoparticle. The barrier to motion is similar to that experienced by polymers in a nanocomposite with hard impenetrable nanoparticles.[33,60] This mechanism leads to a universal dependence of the change in polymer diffusion with nanoparticle inter-particle distance that has been shown to be valid for a broad range of hard nanoparticles.[14] Therefore, comparing the diffusive behavior of the 61k polymers in the presence of the soft nanoparticles to this model provides insight into the relative importance of the entanglement of the polymer and soft nanoparticle and the barrier properties of the nanoparticles on the change in the diffusive behavior of the polymer chain.

However, when the diffusion coefficients of the 61 kDa PS linear polymer chains in the presence of soft nanoparticles are plotted with the universal scaling curve, as in Figure 7, the reduced diffusion coefficients fall below the curve. This is consistent with the interpretation that the slower diffusion is the result of an additional factor beyond the entropic barrier due to nanoparticle confinement. It is our interpretation of these results that this additional factor is the entanglement of the linear polymer with the soft nanoparticles, which further slows the linear polymer chain diffusion.

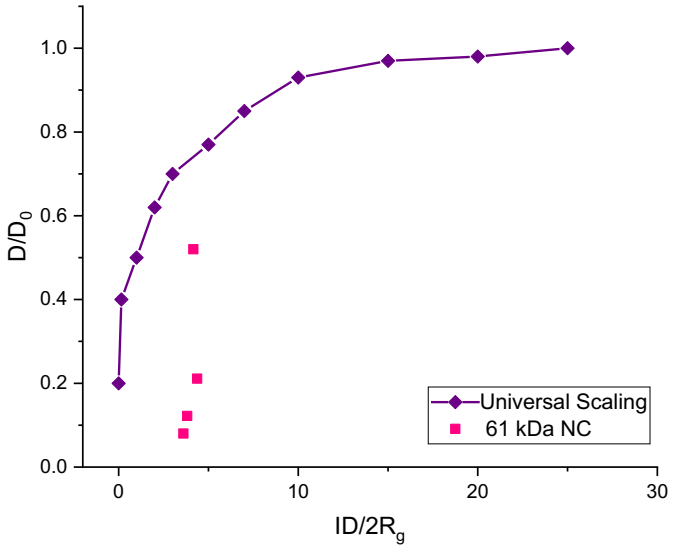

Figure 7: Comparison of 61 kDa nanocomposites to the universal scaling shown in Ref[14].

Diffusion of Polystyrene Nanocomposites: 215k PS Matrix ($R_{g(NP)}$~$R_{g(dPS)}$)

The estimated R_g for linear polystyrene with a molecular weight of 215 kDa is 119 Å using Equation 5. The $R_{g(NP)}$ is now similar in size to that of the $R_{g(dPS)}$ where the ratio of $R_{g(dPS)}/R_{g(NP)}$ is 1.18, 1.74, 1.7, and 1.84 for the NP1, NP2, NP3 and NP4 nanoparticles, respectfully (Figure S 6-10). The 215 kDa linear PS has a diffusion coefficient of 7.4×10^{-16} cm^2/s at 130 °C with a $\tau_{reptation}$ time of 392 seconds. Figure 6 shows that the diffusion coefficients of the neat 215 kDa bilayer and the PS in the nanocomposites are similar, with the NP3 nanocomposite exhibiting the slowest PS diffusion coefficient. At this linear PS molecular weight, the nanoparticles are neither greatly inhibiting nor are they facilitating the diffusion of the linear polystyrene. Simulation studies have suggested that sparsely crosslinked nanoparticles do not confine the linear chains in a nanocomposite.[1] While direct comparison of these simulation results to our experiments is difficult because of variation in the size of the soft nanoparticles, within this simulation study the SCNPs

do not decrease the entanglement length of the linear chain compared to the pure melt as is seen with dense, globular single chain nanoparticles.[1] The lack of change in the length between entanglements in the all-polymer nanocomposite compared to the linear melt results in comparable linear chain dynamics.

At this linear PS molecular weight, the size of the nanoparticle and polymer are comparable. These modest length chains still contain a significant amount of chain ends that provide pathways for the polymer chain to entangle with the soft nanoparticle as in the 61kDa nanocomposites. At the same time, the number of entanglements per chain ($M_w/M_c \approx 6$) suggests that the fuzzy interface of the nanoparticle can also enable constraint release mechanisms in the reptative diffusive motions as found in the 540 kDa PS matrix.[4] Thus, it appears that the slowing down of the polymer diffusion by entanglements or confinement competes with the speeding of the polymer diffusion by constraint release, and that these two factors are nearly equal and cancel each other out at this intermediate molecular weight.

Diffusion of Polystyrene Nanocomposites: 540k PS Matrix ($R_{g(NP)} < R_{g(dPS)}$)

For this set of nanocomposites, the R_g of the linear PS matrix is approximately 190 Å as calculated using Equation 5, which is significantly larger than the nanoparticles. At this molecular weight, the linear polymers have the greatest entanglements per chain ($M_w/M_c \approx 15$). This slows the polymer diffusion significantly, resulting in a diffusion coefficient of 9.4 x 10^{-17} cm^2/s for the neat 540 kDa PS and a $\tau_{reptation}$ of 7803 seconds. Figure 6 however, shows that the diffusion coefficient of the PS chain in the nanocomposite are all faster than that of the neat PS. The PS diffusion coefficient is 3.75 times faster in the NP1 nanocomposite, 2.25 times faster in the NP2 nanocomposite, 1.54 times faster in the NP3 nanocomposite, and 1.2 times faster in the NP4 nanocomposite (Figure S 11-14). This increase in PS diffusion coefficient is only observed in this

matrix molecular weight where the R_g of the PS matrix is greater than that of the polystyrene soft nanoparticles.

Miller et al observed similar behavior and correlated the softness of the nanoparticle to the increase in diffusion coefficients when the R_g of the matrix is larger than that of the nanoparticles.[4] This behavior has been attributed to nanoparticles of this nature supporting constraint release in the reptative polymer diffusion.[3] In this process, the more lightly crosslinked fuzzy interface contains loops and chain ends that behave similarly to the arms of polymer stars. As has been observed in mixtures of star and linear polymers, the retraction and motion of the star's arms increases the release the constraints on the reptation tube, which speeds up the polymer diffusion.[61] The deformability of the nanoparticle allows the relaxation of the nanoparticle, which can enlarge the tube diameter. Thus, the release of the lateral constraints of the linear polymer chains contributes significantly to the overall increase in polymer motion.

This interpretation relies on the chains on the outer surface of the nanoparticle behaving as fast chains that are relaxing faster than the linear polymer chain. A similar tube dilation has been reported for asymmetric mixtures of long poly(ethylene oxide) (PEO) linear chains in the presence of poly(methyl methacrylate) (PMMA) based single-chain nanoparticles using neutron spin echo.[31] The internal compaction of the PMMA nanoparticles in the PEO matrix contributes to the release of entanglements and mechanism of tube dilation. It is interesting that a similar change in soft nanoparticle morphology is observed for our PS nanoparticles when dispersed in a theta solvent.[62]

Effect of Soft Nanoparticles on Nanocomposite Free Volume

To test whether the incorporation of the soft nanoparticles alters the free volume of the polymer, and thus acts as a plasticizer, the glass transition temperature of the nanocomposites was

monitored by differential scanning calorimetry. The results are presented in Figure 8, where the structural characteristics of all soft nanoparticles are provided in Table 1. These results show that the glass transition temperature of the PS in the nanocomposites changes very slightly, and slightly increases, with the addition of the nanoparticles. The neat PS film has a measured T_g of 94.5 °C. When soft nanoparticles are added into the PS matrix, the T_g of all films increased. These results are counter to those of Mackay et al that observed an increase in free volume when highly crosslinked PS nanoparticles are dispersed into a PS matrix, which translates into a decreases in the T_g of the system.[38] However, our system shows an increase in the T_g of the system, which is consistent with a *decrease* in the free volume of the nanocomposite and cannot explain the increase in the diffusion coefficient of the polymer chains. Thus, the unique interfacial structure of these polystyrene soft nanoparticles as well as their softness contribute to the alteration of the polymer diffusion in the nanocomposites.

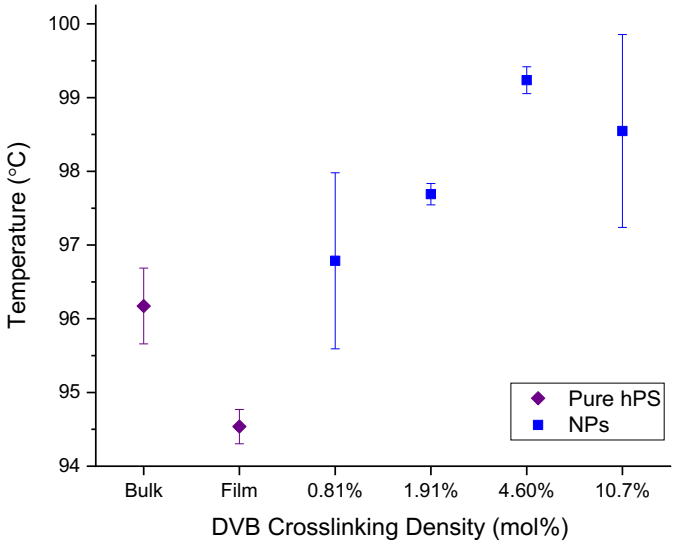

Figure 8: The glass transition temperature of polystyrene and nanocomposites as a function of DVB crosslinker in the nanoparticles.

Conclusion

The results presented above indicate that the relative size of the polymer chain to the soft nanoparticle is a crucial factor in determining the impact of the nanoparticle on the polymer chain diffusion. The addition of the soft penetrable nanoparticle appears to alter the entanglements of the linear polymer. The diffusion of smaller chains is slowed down in the presence of the soft nanoparticles. This behavior is attributed to the topological barrier of the soft nanoparticle and the entanglement of the linear polymer chain with the penetrable soft nanoparticle. At the other end of the spectrum, the presence of the soft nanoparticle speeds up the polymer chain diffusion of the largest polymer. This is ascribed to the facilitation of constraint release of the polymer chain reptation by the fuzzy interface of the soft nanoparticles. Finally, the diffusion of the 215 kDa polymer chain appears to be a balance of these two competing effects such that the rate of diffusion of these polymers does not change much with the addition of the soft nanoparticles. Therefore, the effect of the presence of soft nanoparticles on the diffusion of each polymer can be described as a result of either polymer chain entanglements and topological constraints when the nanoparticle is larger than the polymer chain, constraint-release when the polymer chain is larger than the nanoparticle, or a combination of these phenomena when the size of the polymer and nanoparticle are similar.

Acknowledgements/ Disclaimer

This research was supported by the U.S. Department of Energy, Office of Science, Basic Energy Sciences, Materials Sciences and Engineering Division. The authors acknowledge the support of the National Institute of Standards and Technology, U.S. Department of Commerce, in providing the neutron reflectivity facilities used in this work, where these facilities are supported in part by

the National Science Foundation under Agreement No. DMR-0944772. The identification of commercial products does not imply endorsement by the National Institute of Standards and Technology nor does it imply that these are the best for the purpose. A portion of this research was also completed at ORNL's High Flux Isotope Reactor, which was sponsored by the Scientific User Facilities Division, Office of Basic Energy Sciences, US Department of Energy.

References

(1) Bačová, P.; Lo Verso, F.; Arbe, A.; Colmenero, J.; Pomposo, J. A.; Moreno, A. J. The Role of the Topological Constraints in the Chain Dynamics in All-Polymer Nanocomposites. *Macromolecules* **2017**, *50*, 1719–1731.

(2) Kawaguchi, D.; Nelson, A.; Masubuchi, Y.; Majewski, J. P.; Torikai, N.; Yamada, N. L.; Siti Sarah, A. R.; Takano, A.; Matsushita, Y. Precise Analyses of Short-Time Relaxation at Asymmetric Polystyrene Interface in Terms of Molecular Weight by Time-Resolved Neutron Reflectivity Measurements. *Macromolecules* **2011**, *44* (23), 9424–9433.

(3) Tuteja, A.; Mackay, M. E.; Hawker, C. J.; Van Horn, B. Effect of Ideal, Organic Nanoparticles on the Flow Properties of Linear Polymers: Non-Einstein-like Behavior. *Macromolecules* **2005**, *38* (19), 8000–8011.

(4) Miller, B.; Imel, A. E.; Holley, W.; Baskaran, D.; Mays, J. W.; Dadmun, M. D. The Role of Nanoparticle Rigidity on the Diffusion of Linear Polystyrene in a Polymer Nanocomposite. *Macromolecules* **2015**, *48* (22), 8369–8375.

(5) Kausch, H. H.; Tirrell, M. Polymer Interdiffusion. *Annu. Rev. Mater. Sci.* **1989**, *19* (1), 341–377.

(6) Masaro, L.; Zhu, X. X. Physical Models of Diffusion for Polymer Solutions, Gels and Solids. *Prog. Polym. Sci.* **1999**, *24* (5), 731–775.

(7) Green, P. F.; Kramer, E. J. Matrix Effects on the Diffusion of Long Polymer Chains. *Macromolecules* **1986**, *19* (4), 1108–1114.

(8) Shull, K. R.; Dai, K. H.; Kramer, E. J.; Fetters, L. J.; Antonietti, M.; Sillescu, H. Diffusion by Constraint Release in Branched Macromolecular Matrices. *Macromolecules* **1991**, *24* (2), 505–509.

(9) Karim, A.; Mansour, A.; Felcher, G. P.; Russell, T. P. Short-Time Relaxation at Polymeric Interfaces. *Phys. Rev. B* **1990**, *42* (10), 6846–6849.

(10) Karim, A.; Felcher, G. P.; Russell, T. P. Interdiffusion of Polymers at Short Times. *Macromolecules* **1994**, *27* (23), 6973–6979.

(11) de Gennes, P. G. Reptation of a Polymer Chain in the Presence of Fixed Obstacles. *J. Chem. Phys.* **1971**, *55* (2), 572–579.

(12) Doi, M.; Edwards, S. F. *The Theory of Polymer Dynamics*; Oxford Science, 1986.

(13) Bucknall, D. G.; Butler, S. A.; Higgins, J. S. Studying Polymer Interfaces Using Neutron Reflection. In *Scattering from Polymers*; ACS Symposium Series; American Chemical Society, 1999; Vol. 739, pp 57–73.

(14) Choi, J.; Hore, M. J. A.; Meth, J. S.; Clarke, N.; Winey, K. I.; Composto, R. J. Universal Scaling of Polymer Diffusion in Nanocomposites. *ACS Macro Lett.* **2013**, *2* (6), 485–490.

(15) Choi, J.; Hore, M. J. A.; Clarke, N.; Winey, K. I.; Composto, R. J. Nanoparticle Brush Architecture Controls Polymer Diffusion in Nanocomposites. *Macromolecules* **2014**, *47* (7), 2404–2410.

(16) Tuteja, A.; Mackay, M. E.; Hawker, C. J.; Van Horn, B.; Ho, D. L. Molecular Architecture and Rheological Characterization of Novel Intramolecularly Crosslinked Polystyrene Nanoparticles. *J. Polym. Sci. Part B Polym. Phys.* **2006**, *44* (14), 1930–1947.

(17) Hu, C.; Chen, X.; Chen, J.; Zhang, W.; Zhang, M. Q. Observation of Mutual Diffusion of Macromolecules in PS/PMMA Binary Films by Confocal Raman Microscopy. *Soft Matter* **2012**, *8* (17), 4780–4787.

(18) Composto, R. J.; Kramer, E. J. Mutual Diffusion Studies of Polystyrene and Poly(Xylenyl Ether) Using Rutherford Backscattering Spectrometry. *J. Mater. Sci.* **1991**, *26* (10), 2815–2822.
(19) Eklind, H.; Hjertberg, T. Determination of Interdiffusion in Thin Polymer Films Using FTIR Reflection Absorption Spectroscopy. *Macromolecules* **1993**, *26* (22), 5844–5851.
(20) Imel, A. E.; Rostom, S.; Holley, W.; Baskaran, D.; Mays, J. W.; Dadmun, M. D. The Tracer Diffusion Coefficient of Soft Nanoparticles in a Linear Polymer Matrix. *RSC Adv* **2017**, *7* (25), 15574–15581.
(21) Stamm, M.; Hüttenbach, S.; Reiter, G.; Springer, T. Initial Stages of Polymer Interdiffusion Studied by Neutron Reflectometry. *EPL Europhys. Lett.* **1991**, *14* (5), 451.
(22) Fernandez, M. L., Higgins, J. S.; Penfold, J. Neutron Reflection Studies at Polymer-Polymer Interfaces. *Macromol. Symp.* **1992**, *62* (1), 103–118.
(23) Bucknall, D. G.; Butler, S. A.; Higgins. Real-Time Measurement of Polymer Diffusion Coefficients Using Neutron Reflection - Macromolecules (ACS Publications). *Macromolecules* **1999**, *32* (16), 5453–5456.
(24) Ganguli, S.; Roy, A. K.; Anderson, D. P. Improved Thermal Conductivity for Chemically Functionalized Exfoliated Graphite/Epoxy Composites. *Carbon* **2008**, *46* (5), 806–817.
(25) Nehl, C. L.; Liao, H.; Hafner, J. H. Optical Properties of Star-Shaped Gold Nanoparticles. *Nano Lett.* **2006**, *6* (4), 683–688.
(26) Lin, M.-F.; Kumar Thakur, V.; Jin Tan, E.; See Lee, P. Surface Functionalization of BaTiO 3 Nanoparticles and Improved Electrical Properties of BaTiO 3 /Polyvinylidene Fluoride Composite. *RSC Adv.* **2011**, *1* (4), 576–578.
(27) Evanoff, D. D.; Chumanov, G. Synthesis and Optical Properties of Silver Nanoparticles and Arrays. *ChemPhysChem* **2005**, *6* (7), 1221–1231.
(28) Kim, W.; Zide, J.; Gossard, A.; Klenov, D.; Stemmer, S.; Shakouri, A.; Majumdar, A. Thermal Conductivity Reduction and Thermoelectric Figure of Merit Increase by Embedding Nanoparticles in Crystalline Semiconductors. *Phys. Rev. Lett.* **2006**, *96* (4), 045901.
(29) Wu, C. L.; Zhang, M. Q.; Rong, M. Z.; Friedrich, K. Tensile Performance Improvement of Low Nanoparticles Filled-Polypropylene Composites. *Compos. Sci. Technol.* **2002**, *62* (10–11), 1327–1340.
(30) Jancar, J.; Douglas, J. F.; Starr, F. W.; Kumar, S. K.; Cassagnau, P.; Lesser, A. J.; Sternstein, S. S.; Buehler, M. J. Current Issues in Research on Structure–property Relationships in Polymer Nanocomposites. *Polymer* **2010**, *51* (15), 3321–3343.
(31) Arbe, A.; Pomposo, J. A.; Asenjo-Sanz, I.; Bhowmik, D.; Ivanova, O.; Kohlbrecher, J.; Colmenero, J. Single Chain Dynamic Structure Factor of Linear Polymers in an All-Polymer Nano-Composite. *Macromolecules* **2016**, *49* (6), 2354–2364.
(32) Gam, S.; Meth, J. S.; Zane, S. G.; Chi, C.; Wood, B. A.; Winey, K. I.; Clarke, N.; Composto, R. J. Polymer Diffusion in a Polymer Nanocomposite: Effect of Nanoparticle Size and Polydispersity. *Soft Matter* **2012**, *8* (24), 6512–6520.
(33) Gam, S.; Meth, J. S.; Zane, S. G.; Chi, C.; Wood, B. A.; Seitz, M. E.; Winey, K. I.; Clarke, N.; Composto, R. J. Macromolecular Diffusion in a Crowded Polymer Nanocomposite. *Macromolecules* **2011**, *44* (9), 3494–3501.
(34) Lin, C.-C.; Ohno, K.; Clarke, N.; Winey, K. I.; Composto, R. J. Macromolecular Diffusion through a Polymer Matrix with Polymer-Grafted Chained Nanoparticles. *Macromolecules* **2014**, *47* (15), 5357–5364.

(35) Grabowski, C. A.; Mukhopadhyay, A. Size Effect of Nanoparticle Diffusion in a Polymer Melt. *Macromolecules* **2014**, *47* (20), 7238–7242.
(36) Meth, J. S.; Gam, S.; Choi, J.; Lin, C.-C.; Composto, R. J.; Winey, K. I. Excluded Volume Model for the Reduction of Polymer Diffusion into Nanocomposites. *J. Phys. Chem. B* **2013**, *117* (49), 15675–15683.
(37) Tung, W. S.; Griffin, P. J.; Meth, J. S.; Clarke, N.; Composto, R. J.; Winey, K. I. Temperature-Dependent Suppression of Polymer Diffusion in Polymer Nanocomposites. *ACS Macro Lett.* **2016**, *5* (6), 735–739.
(38) Mackay, M. E.; Dao, T. T.; Tuteja, A.; Ho, D. L.; van Horn, B.; Kim, H.-C.; Hawker, C. J. Nanoscale Effects Leading to Non-Einstein-like Decrease in Viscosity. *Nat. Mater.* **2003**, *2* (November), 762–766.
(39) Tuteja, A.; Mackay, M. E.; Narayanan, S.; Asokan, S.; Wong, M. S. Breakdown of the Continuum Stokes-Einstein Relation for Nanoparticle Diffusion. *Nano Lett.* **2007**, *7* (5), 1276–1281.
(40) Milner, S. T.; McLeish, T. C. B.; Young, R.; Hakiki, A.; Johnson, J. Dynamic Dilution, Constraint-Release, and Star - Linear Blends. *Macromolecules* **1998**, *31*, 9345–9353.
(41) Martin, H. J.; White, B. T.; Scanlon, C. J.; Saito, T.; Dadmun, M. D. Tunable Synthetic Control of Soft Polymeric Nanoparticle Morphology. *Soft Matter* **2017**, *13* (46), 8849–8857.
(42) Hooper, J. B.; Schweizer, K. S. Contact Aggregation, Bridging, and Steric Stabilization in Dense Polymer−Particle Mixtures. *Macromolecules* **2005**, *38* (21), 8858–8869.
(43) Hooper, J. B.; Schweizer, K. S. Theory of Phase Separation in Polymer Nanocomposites. *Macromolecules* **2006**, *39* (15), 5133–5142.
(44) Holley, D. W.; Ruppel, M.; Mays, J. W.; Urban, V. S.; Baskaran, D. Polystyrene Nanoparticles with Tunable Interfaces and Softness. *Polymer* **2014**, *55* (1), 58–65.
(45) Shin, K.; Obukhov, S.; Chen, J.-T.; Huh, J.; Hwang, Y.; Mok, S.; Dobriyal, P.; Thiyagarajan, P.; Russell, T. P. Enhanced Mobility of Confined Polymers. *Nat. Mater.* **2007**, *6* (12), 961–965.
(46) Si, L.; Massa, M. V.; Dalnoki-Veress, K.; Brown, H. R.; Jones, R. A. L. Chain Entanglement in Thin Freestanding Polymer Films. *Phys. Rev. Lett.* **2005**, *94* (12), 127801.
(47) Griffin, P. J.; Bocharova, V.; Middleton, L. R.; Composto, R. J.; Clarke, N.; Schweizer, K. S.; Winey, K. I. Influence of the Bound Polymer Layer on Nanoparticle Diffusion in Polymer Melts. *ACS Macro Lett.* **2016**, *5* (10), 1141–1145.
(48) Lin, C.; Gam, S.; Meth, J. S.; Clarke, N.; Winey, K. I.; Composto, R. J. Do Attractive Polymer-Nanoparticle Interactions Retard Polymer Diffusion in Nanocomposites? *Macromolecules* **2013**, *46* (11), 4502–4509.
(49) Toth, R.; Santese, F.; P. Pereira, S.; R. Nieto, D.; Pricl, S.; Fermeglia, M.; Posocco, P. Size and Shape Matter! A Multiscale Molecular Simulation Approach to Polymer Nanocomposites. *J. Mater. Chem.* **2012**, *22* (12), 5398–5409.
(50) Mu, M.; Clarke, N.; Composto, R. J.; Winey, K. I. Polymer Diffusion Exhibits a Minimum with Increasing Single-Walled Carbon Nanotube Concentration. *Macromolecules* **2009**, *42* (18), 7091–7097.
(51) Chen, T.; Qian, H.-J.; Lu, Z.-Y. Diffusion Dynamics of Nanoparticle and Its Coupling with Polymers in Polymer Nanocomposites. *Chem. Phys. Lett.* **2017**, *687*, 96–100.
(52) Chen, T.; Qian, H.-J.; Zhu, Y.-L.; Lu, Z.-Y. Structure and Dynamics Properties at Interphase Region in the Composite of Polystyrene and Cross-Linked Polystyrene Soft Nanoparticle. *Macromolecules* **2015**, *48* (8), 2751–2760.

(53) Chen, T.; Qian, H.-J.; Lu, Z.-Y. Note: Chain Length Dependent Nanoparticle Diffusion in Polymer Melt: Effect of Nanoparticle Softness. *J. Chem. Phys.* **2016**, *145* (10), 106101.
(54) Mu, M.; Composto, R. J.; Clarke, N.; Winey, K. I. Minimum in Diffusion Coefficient with Increasing MWCNT Concentration Requires Tracer Molecules To Be Larger than Nanotubes. *Macromolecules* **2009**, *42* (21), 8365–8369.
(55) Karatrantos, R.; Composto, R. J.; Winey, K. I.; Kroger, M.; Clarke, N. Entanglements and Dynamics of Polymer Melts near a SWCNT. *Macromolecules* **2012**, *45*, 7273–7281.
(56) Tuteja, A.; Duxbury, P. M.; MacKay, M. E. Polymer Chain Swelling Induced by Dispersed Nanoparticles. *Phys. Rev. Lett.* **2008**, *100* (7), 21–24.
(57) Imel, A. E. Polymer Additives Effects on Structure and Dynamics. **2015**.
(58) Antonietti, M.; Coutandin, J.; Sillescu, H. Diffusion of Linear Polystyrene Molecules in Matrixes of Different Molecular Weights. *Macromolecules* **1985**, *19* (3), 793–798.
(59) Antonietti, M.; Sillescu, H. Diffusion of Intramolecular Crosslinked and Three-Arm-Star Branched Polystyrene Molecules in Different Matrixes. *Macromolecules* **1986**, *19* (3), 798–803.
(60) Muthukumar, M.; Baumgaertner, A. Effects of Entropic Barriers on Polymer Dynamics. *Macromolecules* **1989**, *22* (4), 1937–1941.
(61) Shivokhin, M. E.; van Ruymbeke, E.; Bailly, C.; Kouloumasis, D.; Hadjichristidis, N.; Likhtman, A. E. Understanding Constraint Release in Star/Linear Polymer Blends. *Macromolecules* **2014**, *47* (7), 2451–2463.
(62) Martin, H. J.; White, B. T.; Wang, H.; Mays, J. W.; Saito, T.; Dadmun, M. D. Effect of Solvent Quality and Monomer Water Solubility on Soft Nanoparticle Morphology in *Gels and Other Soft Amorphous Solids* F. Horkay, Ed., ACS Symp. Ser. 1269, ACS Books (2018).